Supporting Information

Atomic Mechanism of Strain Alleviation and Dislocation Reduction in Highly Mismatched Remote Heteroepitaxy Using a Graphene Interlayer

Bingyao Liu[a,b,c,d§], Qi Chen[e,f§], Zhaolong Chen[c,d,g§], Shenyuan Yang[f,h]*, Jingyuan Shan[c,d], Zhetong Liu[a,b,c,d], Yue Yin[e,f], Fang Ren[e,f], Shuo Zhang[e,f], Rong Wang[d], Mei Wu[a], Rui Hou[f,h], Tongbo Wei[e,f], Junxi Wang[e,f], Jingyu Sun[d,i], Jinmin Li[e,f], Zhongfan Liu[c,d]*, Zhiqiang Liu[e,f]*, Peng Gao[a,b,d,j]*.

[a] *Electron Microscopy Laboratory, and International Center for Quantum Materials, School of Physics, Peking University, Beijing 100871, China.*

[b] *Academy for Advanced Interdisciplinary Studies, Peking University, Beijing 100871, China.*

[c] *Center for Nanochemistry (CNC), Beijing Science and Engineering Center for Nanocarbons, Beijing National Laboratory for Molecular Sciences, College of Chemistry and Molecular Engineering, Peking University, Beijing 100871, China.*

[d] *Beijing Graphene Institute (BGI), Beijing 100095, China.*

[e] *Research and Development Center for Semiconductor Lighting Technology, Institute of Semiconductors, Chinese Academy of Sciences, Beijing 100083, China.*

[f] *Center of Materials Science and Optoelectronics Engineering, University of Chinese Academy of Sciences, Beijing 100049, China.*

[g] *Institute for Functional Intelligent Materials, National University of Singapore, 117544, Singapore.*

[h] *State Key Laboratory of Superlattices and Microstructures, Institute of Semiconductors, Chinese Academy of Sciences, Beijing 100083, China.*

[i] *College of Energy, Soochow Institute for Energy and Materials Innovations, Jiangsu Provincial Key Laboratory for Advanced Carbon Materials and Wearable Energy Technologies, Soochow University, Suzhou 215006, China.*

[j] *Collaborative Innovation Center of Quantum Matter, Beijing 100871, China.*

*Email: syyang@semi.ac.cn; zfliu@pku.edu.cn; lzq@semi.ac.cn; p-gao@pku.edu.cn.

§ B. L., Q. C. and Z. C. contributed equally to this paper.

1. METHODS

CVD growth of graphene films over sapphire substrates: 10 pieces of commercial *c*-sapphire substrate were placed on a home-made substrate holder (**Figure S1**) and then loaded into a high-temperature furnace. The graphene growth was performed at atmospheric pressure with 800 sccm Ar, 600 sccm H_2, and 50 sccm CH_4 at 1080 °C for 5 h.

MOCVD process of the yellow LED: We did not use any plasma treatment during the whole process to prevent any severe damage to the graphene. Trimethylgallium (TMGa) and trimethylaluminum (TMAl) were used as Ga and Al precursors for the epitaxy of GaN and $Al_xGa_{1-x}N$ ($Al_{0.1}Ga_{0.9}N$) layers, respectively; triethylgallium (TEGa) and trimethylindium (TMIn) were used as Ga and In precursors for the epitaxy of $In_xGa_{1-x}N$/GaN MQWs, respectively; and NH_3 was used as the N precursor during the whole process. First, the high-temperature $Al_{0.1}Ga_{0.9}N$ buffer layer (100 nm) was grown at a set temperature of 1030 °C with NH_3 flow of 30 slm, TMGa flow of 55 sccm, and TMAl flow of 25 sccm. Subsequently, the temperature was raised to 1078 °C and the flow was adjusted for u-GaN growth. Then, a thick u-GaN layer (4 μm) was grown at 1133 °C with NH_3 flow of 65 slm, TMGa flow of 661 sccm, followed by a n-doped GaN layer (2 μm) with the silicane flow of 12.5 sccm. Then, 5 periods of $In_xGa_{1-x}N$ (3 nm)/GaN (13 nm) active layers were grown at the nominal temperature of 758.5 °C/895 °C with the switched TMIn of 485 sccm. A p-layer (120 nm) was further deposited at 950 °C with bis-cyclopentadienyl magnesium (Cp_2Mg) flow of 400/200/500 sccm.

Electron microscopy characterizations and analysis: The cross-sectional TEM sample was made by ThermoFisher Helios G4 UX focused ion beam system. The HAADF, iDPC, and EDS mapping were performed using FEI Titan Cubed Themis G2 300 spherical aberration corrected STEM, operated at 300 kV. The convergence semi angle was 30 mrad and the collection semi angles of HAADF and iDPC were 39 to 200 mrad and 4 to 21 mrad, respectively. The camera length in HAADF and iDPC modes were set as 145 and 360 mm, respectively. SAED was performed using FEI Tecnai F20 TEM, operated at 200 kV. The diameter of aperture was set to be 200 nm. The SEM images and CL spectrum were taken on FEI Quanta 200F field-emission SEM, equipped with a Gatan MonoCL detector. The HAADF and iDPC images were

filtered with block matching and 3-D filtering method[1]. The contrast in **Figure 1a** is sqrt for better contrast.

Spectroscopy characterizations: Raman spectra were taken using LabRAM HR Evolution Raman microscopy with 532 nm laser excitation, while XRD spectra were recorded using D8 Discover High-resolution XRD system with Cu K α radiation, $\lambda \sim 1.5418$ Å.

Computational details: The first-principles calculations based on DFT was performed using the Vienna ab-initio simulation package (VASP)[2] with the generalized-gradient approximation of Perdew, Burke, and Ernzerhof (PBE)[3] for the exchange correlation functional. We used the all-electron-like projector-augmented wave potentials[4] and set the energy cutoff for the plane-wave expansion as 400 eV. Weak van der Waals (vdW) interactions were included with the Becke88 optimization (optB88) functional[5]. The Al-terminated □-Al_2O_3 (0001) surface was modeled using an eight-layer slab with the bottom passivated by pseudo-hydrogen atoms. To model the graphene/sapphire interface, the graphene 2×2 cell with a compressive strain of 2.75% was matched to sapphire 1×1 surface cell. At the AlGaN/Gr/sapphire interface, TEM showed that both low-Al and high-Al atoms are presented at the interface. Our simulated interface structure with low-Al, high-Al, and an O atom on top of low-Al atom agrees well with the TEM image. The distance between the high-Al and the graphene layer was calculated to be 3.53 Å, which is in good agreement with the experimental value. In GaN/graphene interface, the N-terminated GaN (0001) surface was modeled using a six-bilayer slab with the bottom passivated by pseudo-hydrogen atoms. The graphene 4×4 cell was matched to GaN (0001) 3×3 surface cell.

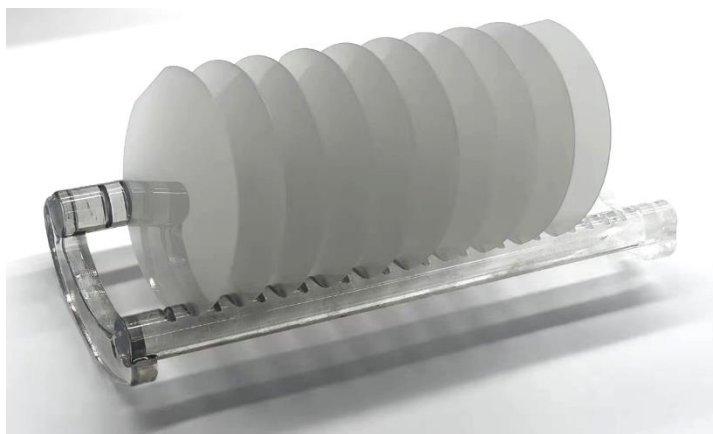## 2. Batch synthesized graphene/sapphire composite substrates

Figure S1. Photo of the batch synthesized graphene/sapphire composite substrates.
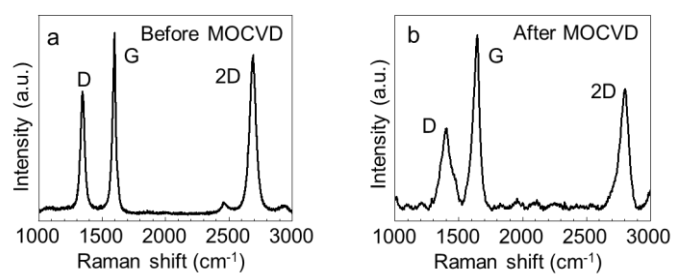
3. Raman spectra of graphene

Figure S2. Raman spectra before **a)** and after **b)** MOCVD process.
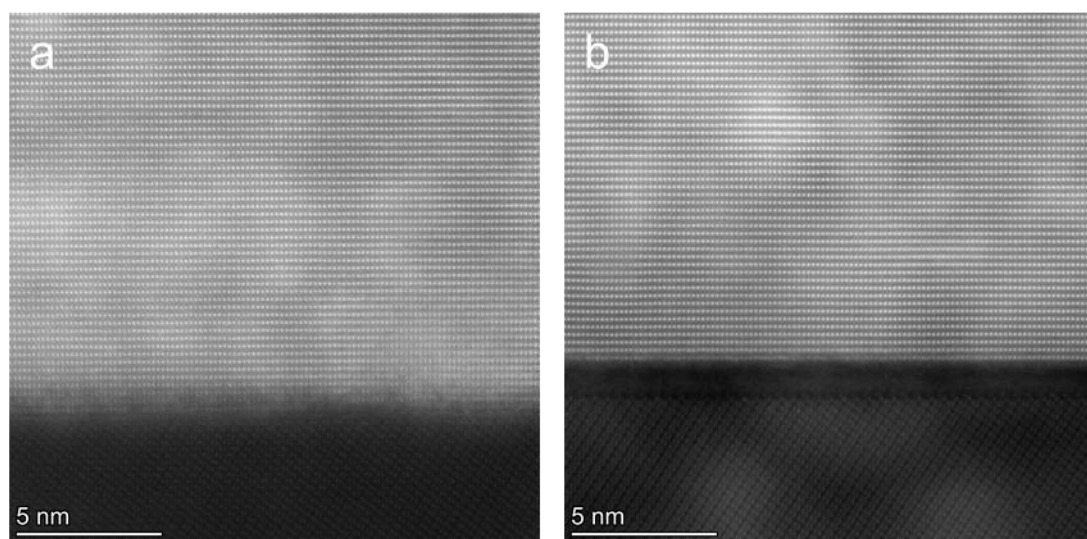
4. Atomic characterizations of the interface

Figure S3. HAADF images of AlGaN/sapphire interface without **a)** and with **b)** graphene.

5. Calculations of the lattice mismatch

On $[1\bar{1}00]$ AlGaN $\parallel$ $[2\bar{1}\bar{1}0]$ sapphire zone axis, the degree of lattice mismatch according to sapphire can be estimated by[6]:

$$\Delta = \frac{d_{\text{M-M, AlGaN } [1\bar{1}00]} - d_{\text{Al-Al, sapphire } [2\bar{1}\bar{1}0]}}{d_{\text{Al-Al,sapphire } [2\bar{1}\bar{1}0]}} \tag{1}$$

where the $d_{\text{Al-Al, sapphire } [2\bar{1}\bar{1}0]}$ is the horizonal distance between two vertical Al atom columns in sapphire $[2\bar{1}\bar{1}0]$ zone axis, has a fixed value of 1.3712 Å; and the $d_{\text{M-M, AlGaN } [1\bar{1}00]}$ is the horizonal distance between two vertical metal atom columns in AlGaN $[1\bar{1}00]$ zone axis, varying with the stains in epilayer.

According to Vegard's Law[7], in strain-free $Al_{0.1}Ga_{0.9}N$, $d_{\text{M-M,AlGaN}[1\bar{1}00]}$ is 1.5951 Å, so the lattice mismatch in strain free AlGaN is 16.3%.

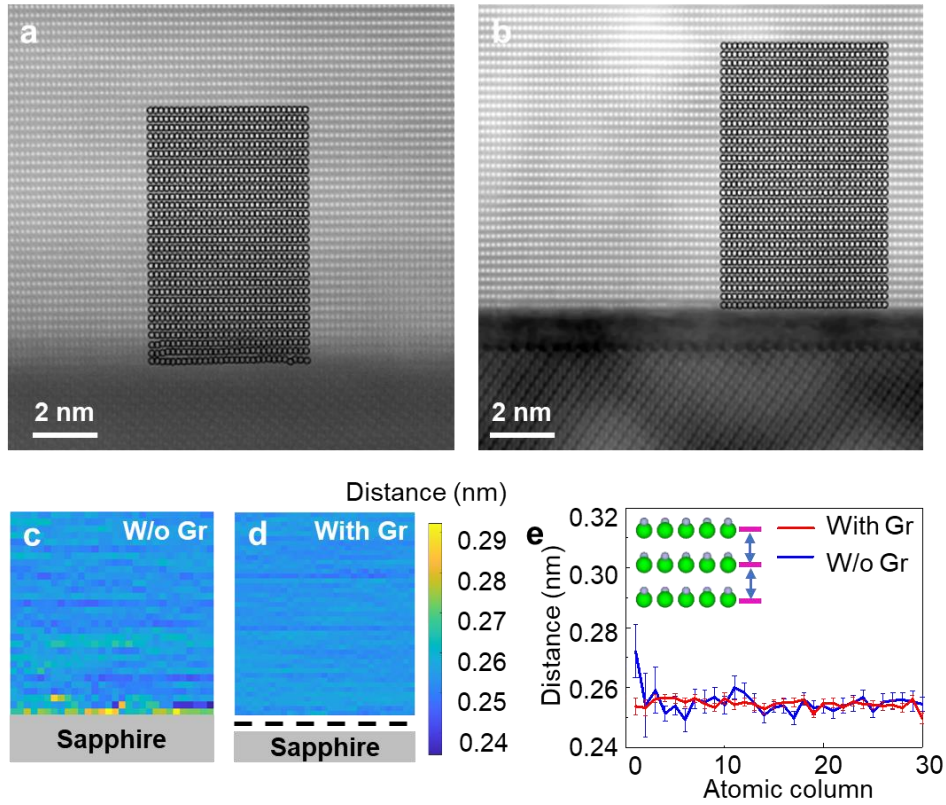## 6. Out of plane lattice fluctuations

Figure S4 Analysis about surface out of plane tensile strain induced by in-plane strain. **a-b)** HAADF images of nitrides on sapphire without and with graphene, respectively. The black circles indicate the atom position located by two-dimensional Gaussian peaks simultaneously fitting. **c-d)** Mapping of calculated distance between two adjacent atoms in c-direction without and with graphene, respectively, corresponding to the black circles shadowed area. **e)** Statistics of the average atomic c-plane distance. Blue: without graphene; Red: with graphene. Inset: schematic of atom layer distance in c-direction. The green and light blue balls represent Ga and N atoms.

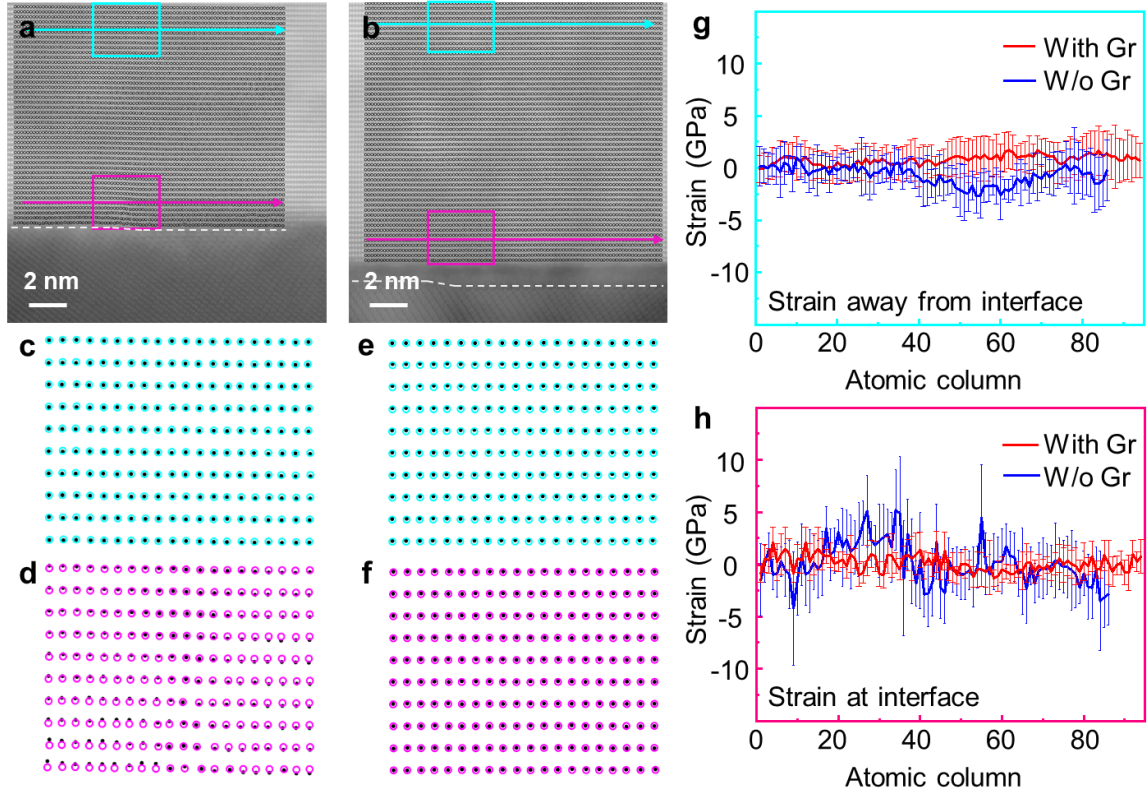## 7. Calculations about the offset and strains near steps

Figure S5 Atom offset and local strains reduced by the steps on sapphire. **a-b)** HAADF images about nitride on sapphire step without and with graphene, respectively. **c-d)** Atom offset away from and near the interface without graphene, respectively. **e-f)** Atom offset away from and near the interface with graphene, respectively. Cyan circle: simulated no strain atom position away from the interface; pink circle: simulated no strain atom position near the interface; black dot: real atom position. **g-h)** Calculated out of plane strains dispersion away from **g)** and near **h)** the interface, respectively. Red: with graphene; blue: without graphene.

We label the atom in this area by

A_{00} $\qquad\qquad$ A_{01}

A_{10} $\qquad\qquad$ A_{11}

$$\ldots\ldots$$

$$A_{ij}$$

where the coordinate of atom is A_{ij} (X_{ij}, Y_{ij}).

We suppose that the top most layer is almost free from strains from the steps. The coordinate of atom in this layer is A_{0j} (X_{0j}, Y_{0j}). We use the average distance $\bar{l}$ between each two adjacent atoms in c-direction to be the standard no strain distance between c-planes:

$$\bar{l} = \sum_{i,j} \frac{Y_{i+1,j} - Y_{i,j}}{i \times (j-1)}$$

because even at the step area, the area with compressive and tensile strains should compensate the influence to the average from each other. Then we can simulate in no strain film, atom position should be A_{ij} $(X_{0j}, Y_{0j}+i\bar{l})$, which is labeled by circles in **figure S5c-f**. However, the real atom position of is A_{ij}' (X_{ij}', Y_{ij}'), which is labeled by dots in **figure S5c-f**. Then the atom offset in c-direction is:

$$\Delta Y = Y_{ij}' - (Y_{0j} + i\bar{l})$$

We can see an obvious offset in **figure S5d**, corresponding to the no graphene step area, while no obvious offset occurs in the case with graphene or in the area away from no graphene interface.

According to Vegard's law, the elastic modulus of $Al_xGa_{1-x}N$ should be[8]:

$$E_{AlxGa1-xN} = xE_{AlN} + (1-x)E_{GaN}$$

For $Al_{0.1}Ga_{0.9}N$ in our case, elastic modulus E in c-direction is estimated to be 280 GPa[9]. The local strain in c-direction can be estimated by:

$$S_{ij} = E \times \frac{Y_{i+1,j} - Y_{i,j}}{\bar{l}}$$

The strains stay stable in both cases away from the interface (**figure S5g**). The difference happens at the interface. There is a huge strain fluctuation (around -2~5 GPa) near the step on bare sapphire, while the strain still keeps stable on graphene paved step (**figure S5h**).

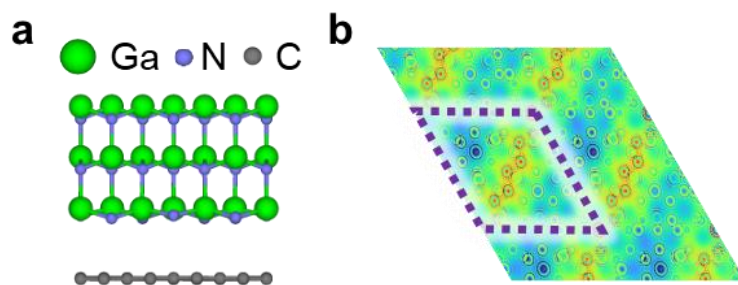## 8. Surface potential of monolayer graphene covered GaN

Figure S6. a) Model of the simulated structure, in which the green, light blue, and grey balls represent Ga, N, and C atoms, respectively. **b)** Calculated surface potential of the monolayer graphene covered GaN.
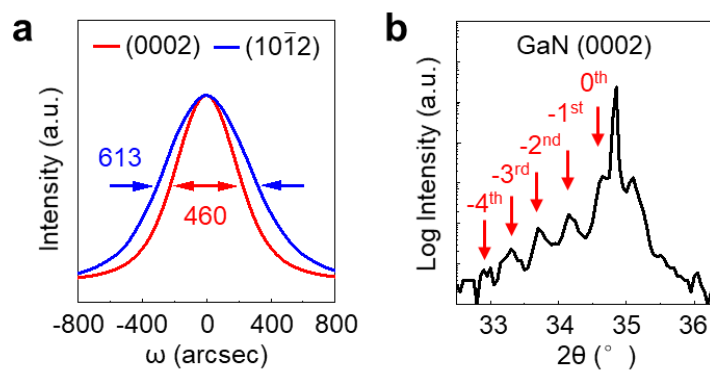
9. XRD of the as-grown GaN film and MQWs

Figure S7. a) XRD rocking curves around (0002) (red) and $(10\bar{1}2)$ (blue) peaks from epitaxial GaN films without graphene. **b)** XRD 2θ scan around GaN (0002) peak.

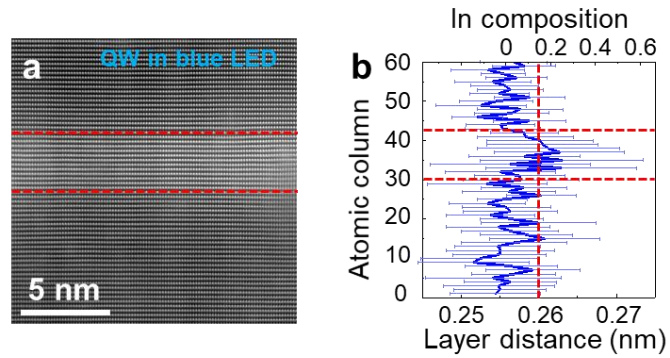## 10. In composition measurement of a traditional blue LED

Figure S8. a) Atomic resolution HAADF image of one period of InGaN/GaN QW in a traditional blue LED. **b)** Statistics of the c-layer distances along out-of-plane direction in **a)**. The horizonal dashed lines highlight the InGaN wells, while the vertical dashed lines indicate the average In composition at these areas.

References

(1) Dabov, K.; Foi, A.; Katkovnik, V.; Egiazarian, K. Image Denoising by Sparse 3-D Transform-Domain Collaborative Filtering. *IEEE Transactions on Image Processing* **2007**, *16* (8), 2080–2095. https://doi.org/10.1109/TIP.2007.901238.

(2) Kresse, G.; Hafner, J. *Ab Initio* Molecular Dynamics for Liquid Metals. *Phys. Rev. B* **1993**, *47* (1), 558–561. https://doi.org/10.1103/PhysRevB.47.558.

(3) Perdew, J. P.; Burke, K.; Ernzerhof, M. Generalized Gradient Approximation Made Simple. *Phys. Rev. Lett.* **1996**, *77* (18), 3865–3868. https://doi.org/10.1103/PhysRevLett.77.3865.

(4) Blöchl, P. E. Projector Augmented-Wave Method. *Phys. Rev. B* **1994**, *50* (24), 17953–17979. https://doi.org/10.1103/PhysRevB.50.17953.

(5) Klimeš, J.; Bowler, D. R.; Michaelides, A. Van Der Waals Density Functionals Applied to Solids. *Phys. Rev. B* **2011**, *83* (19), 195131. https://doi.org/10.1103/PhysRevB.83.195131.

(6) Wang, M. X.; Xu, F. J.; Xie, N.; Sun, Y. H.; Liu, B. Y.; Ge, W. K.; Kang, X. N.; Qin, Z. X.; Yang, X. L.; Wang, X. Q.; Shen, B. High-Temperature Annealing Induced Evolution of Strain in AlN Epitaxial Films Grown on Sapphire Substrates. *Appl. Phys. Lett.* **2019**, *114* (11), 112105. https://doi.org/10.1063/1.5087547.

(7) Kuo, Y.-K.; Liou, B.-T.; Yen, S.-H.; Chu, H.-Y. Vegard's Law Deviation in Lattice Constant and Band Gap Bowing Parameter of Zincblende InxGa1−xN. *Optics Communications* **2004**, *237* (4–6), 363–369. https://doi.org/10.1016/j.optcom.2004.04.012.

(8) Amar, A. B.; Faucher, M.; Brandli, V.; Cordier, Y.; Théron, D. Young's Modulus Extraction of Epitaxial Heterostructure AlGaN/GaN for MEMS Application. *physica status solidi (a)* **2014**, *211* (7), 1655–1659. https://doi.org/10.1002/pssa.201330339.

(9) Wright, A. F. Elastic Properties of Zinc-Blende and Wurtzite AlN, GaN, and InN. *Journal of Applied Physics* **1997**, *82* (6), 2833–2839. https://doi.org/10.1063/1.366114.